JOURNAL OF CATALYSIS **151**, 17–25 (1995)

In Situ XAFS Investigation of K-Promoted Co Catalysts

Gerald P. Huffman,* Naresh Shah,* Jianmin Zhao,* Frank E. Huggins,* T. Eddy Hoost,†
Siri Halvorsen,†,[1] and James G. Goodwin, Jr.†

**Consortium for Fossil Fuel Liquefaction Science, 341 Bowman Hall, University of Kentucky, Lexington, Kentucky 40506-0059; and*
†Department of Chemical and Petroleum Engineering, University of Pittsburgh, Pittsburgh, Pennsylvania 15261

Received January 11, 1994; revised August 18, 1994

In situ XAFS spectroscopy studies have been conducted at reaction conditions on potassium-promoted cobalt catalysts supported on SiO_2 and Al_2O_3, and on similar samples without potassium. Measurements were conducted at temperature up to 200°C under both reducing (flowing H_2) and simulated Fischer–Tropsch (F–T) reaction (flowing CO/H_2) conditions. K and Co K-edge XANES spectra indicate that K interacts with both the Co phase and the SiO_2 support, and that K promotion inhibits the reduction of the Co/SiO_2 catalyst in H_2 at 200°C. However, under CO hydrogenation conditions in the presence of water vapor, the differences in degree of reducibility are less since the unpromoted catalyst becomes more oxidized. For the K-promoted Co/Al_2O_3 catalyst, Co K-edge XANES and EXAFS spectra show that Co is initially present as a mixture of Co_3O_4 and CoO. Under H_2 at 200°C, these oxides are reduced to a mixture of CoO and Co metal. During reaction at 200°C in H_2/CO, the Co phases are reconverted to a mixture of Co_3O_4 and CoO. Without K, the Co in Co/Al_2O_3 is reduced almost completely to Co metal under H_2 at 200°C and remains in that form even during reaction at 200°C in H_2/CO. Only a minor trace of CoO is observed.

INTRODUCTION

Promoters such as potassium are known to enhance the selectivity of Fischer–Tropsch (F–T) catalysts for the production of longer chain hydrocarbons from synthesis gas. There is little understanding, however, of how such promoters work, and, in particular, how they might modify the structure of the catalysts, because most studies have been limited to the examination of the state of the catalysts in their as-prepared state or their final state after the completion of the syngas reaction using such techniques as XRD, XPS, or Mössbauer spectroscopy (1, 2). *In situ* measurements by FT-IR have been carried out during CO hydrogenation on various catalysts (3–5); however, such measurements permit only indirect conclusions about the state of the catalyst itself. To date, as far as can be discerned, no paper in the literature has reported results for an investigation by X-ray absorption fine structure (XAFS) of the catalyst itself during CO hydrogenation.

XAFS spectroscopy has developed over the past several years into an excellent probe for determining catalyst structures (6–11). In particular, a number of groups have succeeded in using this technique for *in situ* investigations of catalyst structures and reactions. This paper reports an investigation using *in situ* XAFS spectroscopy to study K-promoted Co catalysts supported on SiO_2 and Al_2O_3 during high-temperature reduction in hydrogen and subsequent reaction in a synthesis gas mixture.

II. EXPERIMENTAL

A 9.0 wt% Co/Al_2O_3 catalyst was prepared by impregnating alumina with an aqueous solution of Co nitrate under incipient wetness conditions. The catalyst precursor was then dried at 33°C and 4.8×10^{-3} atm for 96 h, calcined in a 150 cc/min flow of air by heating at 5°C/min from room temperature to 350°C, and remaining at that temperature for 2 h. The calcined material was then reduced in a 100 cc/min flow of H_2 at 350°C for 5 h. Following reduction, the catalyst was passivated by contacting it slowly with oxygen. This catalyst has a BET surface area of 150 m^2/g. The weight loading of Co was confirmed by elemental analysis.

The K-promoted Co/Al_2O_3 catalyst was prepared by impregnating the passivated 9.0 wt% Co/Al_2O_3 catalyst with a solution of potassium nitrate in order to have an atomic ratio of K/Co = 1. This catalyst was then dried at 100°C overnight, reduced in a 100 cc/min flow of hydrogen while heating from room temperature to 350°C at 1.8°C/min, and remaining for 5 h at 350°C before being passivated at room temperature. Impregnating the catalyst with the promoter after the calcination and initial reduction of the supported Co minimizes possible differences in the Co particle size distribution. While the presence of alkali species during catalyst preparation can affect this distribution, significant differences in particle

---

[1] Permenant address: Center for Industiforskning, Oslo, Norway.

0021-9517/95 $6.00

size distribution could act to confuse interpretation of any chemical effect of the promoter on the reaction characteristics and the final state of the metal.

Unpromoted and K-promoted (K/Co = 1) 4.4 wt% Co/SiO_2 catalysts were prepared in a similar manner except that they were initially dried at 120°C for 8 h. The Co/SiO_2 catalyst had a BET surface area of 260 m^2/g.

XAFS experiments were carried out at beam-line X-19A at the National Synchrotron Light Source (NSLS) at Brookhaven National Laboratory. Experiments were performed using a Si(111) double-crystal monochromator to vary the X-ray energy across the potassium K-edge, and a Si(220) double-crystal monochromator to investigate the cobalt K-edge. The X-ray energy was normally varied from approximately 100 eV below to several hundred eV above the edges of interest. To eliminate higher reflection harmonics, the monochromator was detuned by 60–70% at the K K-edge, and by 40–50% at the Co K-edge.

The *in situ* XAFS measurement system (Fig. 1) was originally designed by Lytle *et al.* (12, 13) and has been extensively used by this group to investigate coal gasification and coal liquefaction catalysts (9–11). The sample chamber was redesigned to consist of a stainless steel cell sealed by a 10 micron beryllium window with a copper gasket. The reactant gas (either H_2 or a CO–H_2 mixture) flowed into and out of the cell via stainless steel tubes in the top of the cell. The larger chamber in which the sample cell sat was filled with helium. This design reduces X-ray absorption and improves the signal-to-noise ratio,

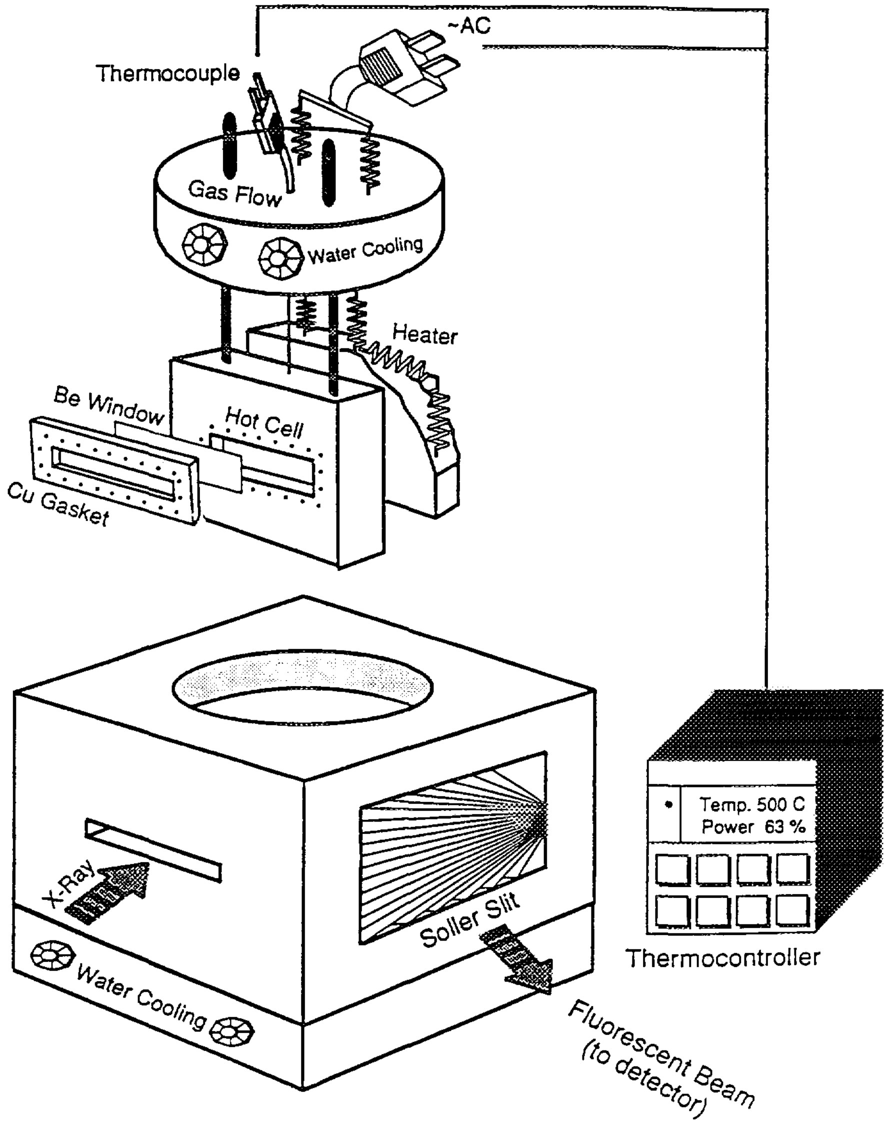

FIG. 1. Schematic of the *in situ* XAFS reaction system.

particularly for the lower energy potassium K-edge measurements.

The sequence of *in situ* treatments and XAFS measurements for the catalysts was as follows: (1) room temperature [XAFS]; (2) 20 min at 80°C in flowing H_2; (3) 20 min at 120°C in flowing H_2; (4) 20 min at 200°C in flowing H_2 [XAFS]; (5) 1 h at 190–200°C in $1CO + 3H_2$ [XAFS]; (6) 1 h at 190–200°C in $1CO + 3H_2$ saturated with H_2O vapor at 25°C [XAFS]; (7) cool down to room temperature [XAFS]. While no on-line analysis of the gas emanating from the sample cell was made, gas samples were collected in evacuated glass containers for selected runs. GC/MS analysis of these samples confirmed that the desired F–T synthesis took place in the XAFS sample cell.

III. RESULTS AND DISCUSSION

Potassium K-Edge XANES

Figure 2 shows the potassium K-edge X-ray absorption near edge structure (XANES) spectra of several potassium model compounds at room temperature. The XANES spectra are dominated by two major peaks: peak *a* at $\sim$3 eV is referred to as the "white line" and represents the $1s \rightarrow np$ transition, whereas peak b_1 or b_2 is the result of multiple scattering resonance. For KOH and K_2CO_3, peak b_2 is found to be at 9–10 eV, whereas b_1 for the three potassium silicates occurs at 7–8 eV. All three peaks, *a*, b_1, and b_2 are observed in the *in situ* XANES spectra for the K-promoted 4.4% Co/SiO_2 catalyst, as shown in Fig. 3. Peak b_2 becomes more prominent after reaction. Upon comparison with the XANES spectra of the model compounds, it appears that the potassium is present in two phases: in one, potassium reacts with the SiO_2 support to form a silicate, and in the other, potassium occurs in an oxide of simple structure. The latter is likely to be incorporated at or near the surface of the Co phase.

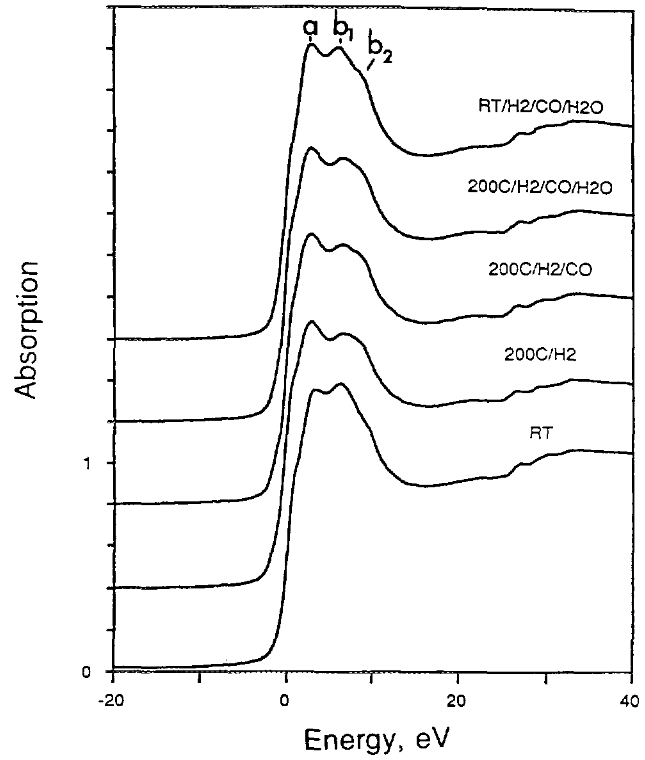

FIG. 3. *In situ* K K-edge XANES spectra obtained from the K-Co/SiO_2 catalyst (4 wt% Co, with K/Co $\sim$1).

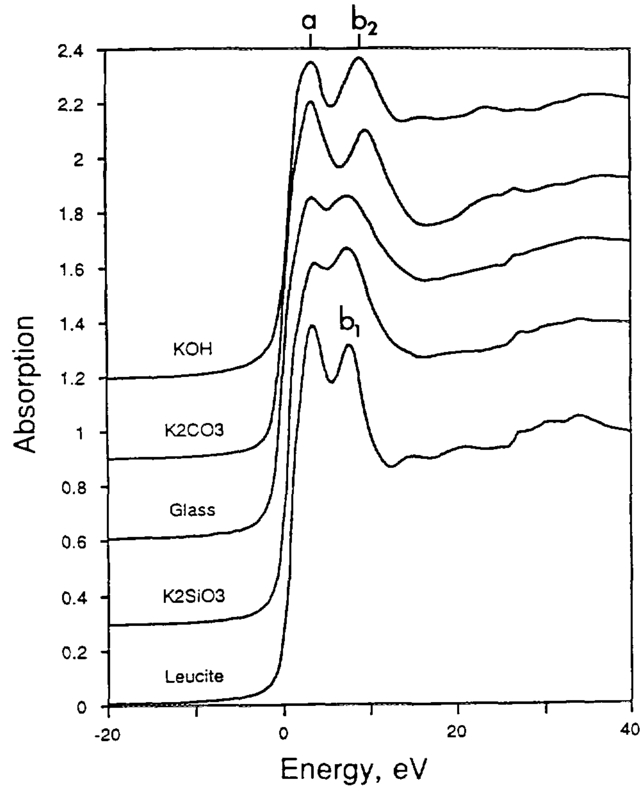

FIG. 2. K K-edge XANES spectra of several model compounds.

Cobalt K-Edge XANES

The XANES spectra of Co metal and Co_3O_4 are shown in Fig. 4. The spectrum for Co_3O_4 shows a preedge peak below the absorption edge which is assigned to the $1s \rightarrow 3d$ transition and a sharp peak above the edge derived from the $1s \rightarrow np$ transition (white line). These features have been observed in most transition metal oxides. The XANES spectrum for Co metal shows a big shoulder at the edge, but no white line.

Figure 5 shows the *in situ* XANES of the 4.4% Co/SiO_2 with potassium promotion. Upon exposing the prereduced/passivated K-promoted Co/SiO_2 catalyst to H_2 at 200°C, there is little or no reduction, and further treat-

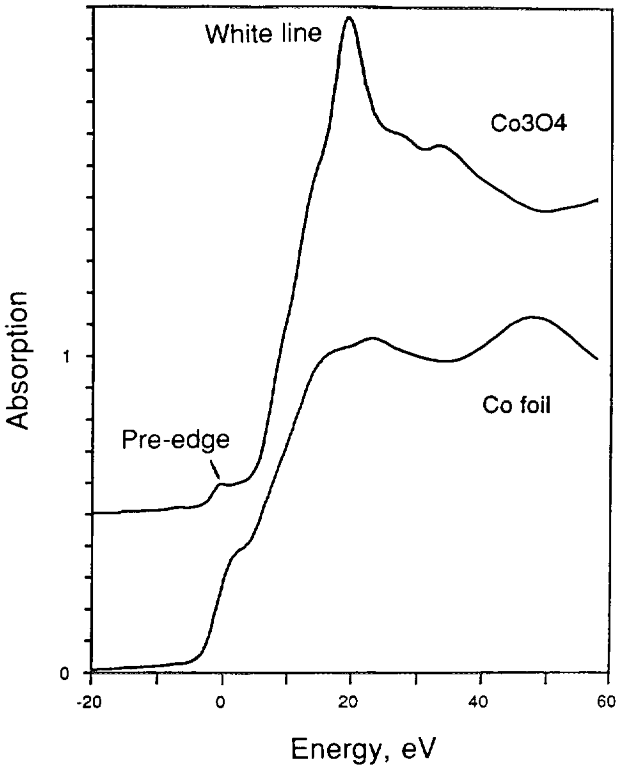

FIG. 4. Co K-edge XANES spectra of Co model compounds.

ments produce no significant changes. Without K promotion (Fig. 6), however, there is a total reduction of Co to its metallic state upon exposure to H_2 at 200°C and Co remains metallic after exposure to Co/H_2 at 200°C, as indicated by the shoulder at the absorption edge. When H_2/CO is bubbled through water to introduce excess water vapor into the reaction cell, the spectra indicate some oxidation of Co as shown by the enhancement of the white line. Because of the design of the X-19A beam lines at NSLS, only the XANES region of the Co K-edge XAFS spectra could be collected while using the Si(111) monochromator setting.

XAFS spectra using the Si(220) monochromator setting were collected in order to examine the 9 wt% Co/Al_2O_3 catalysts with and without K promoting. In this setup, the monochromator can cover the Co K-edge EXAFS region, but it is unable to reach the potassium K-edge. Figure 7 shows the *in situ* Co K-edge XANES for the K-promoted 9 wt% Co/Al_2O_3 catalyst. There is some reduction of Co at 200°C under H_2, as indicated by the shoulder at the absorption edge; however, the reduced Co phase becomes oxidized when H_2/CO is introduced. Figure 8 shows the *in situ* Co K-edge XANES for the Co/Al_2O_3 catalyst without K. Unlike the 4.4 wt% Co/SiO_2 sample (Fig. 6), in which Co is reduced entirely to Co metal in H_2 at 200°C, there appears to be a small fraction

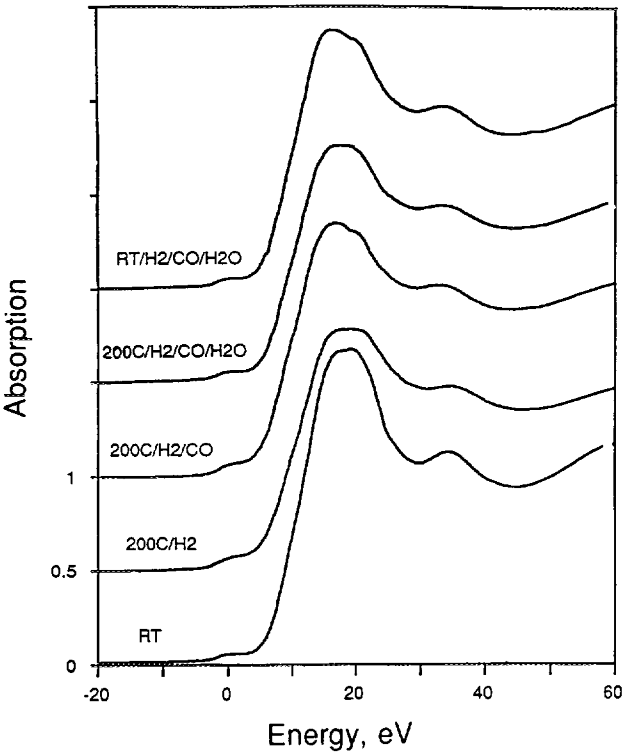

FIG. 5. *In situ* Co K-edge XANES spectra of the K–Co/SiO_2 catalyst (4.4 wt% Co, with K/Co ~1).

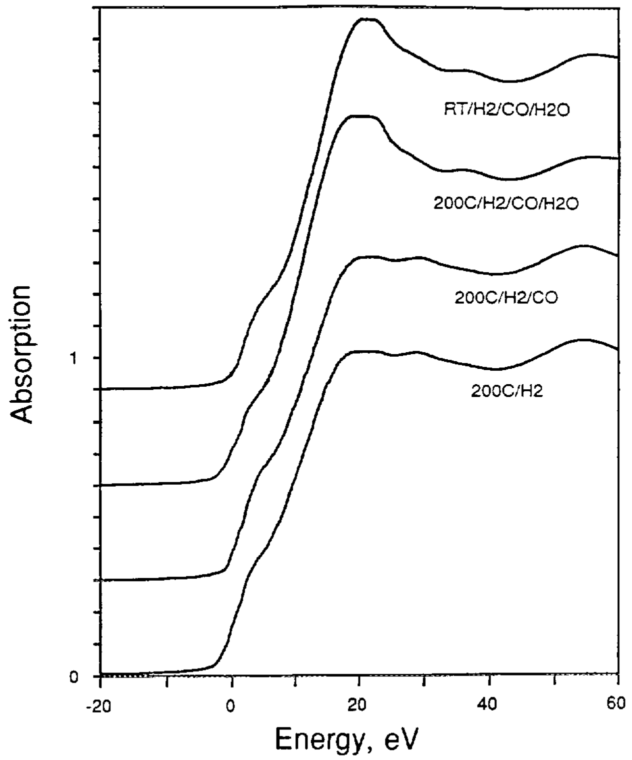

FIG. 6. *In situ* Co K-edge XANES spectra of the Co(4.4 wt%)/SiO_2 catalyst without K.

of Co oxide forms present even after exposure to hydrogen at 200°C. This may be due to formation of Co aluminate ($CoAl_2O_4$). Further treatments do not produce significant changes. The results suggest that in the presence of K, the Co/Al_2O_3 catalyst becomes less easy to reduce, suggesting that potassium K is likely incorporated with the Co phase.

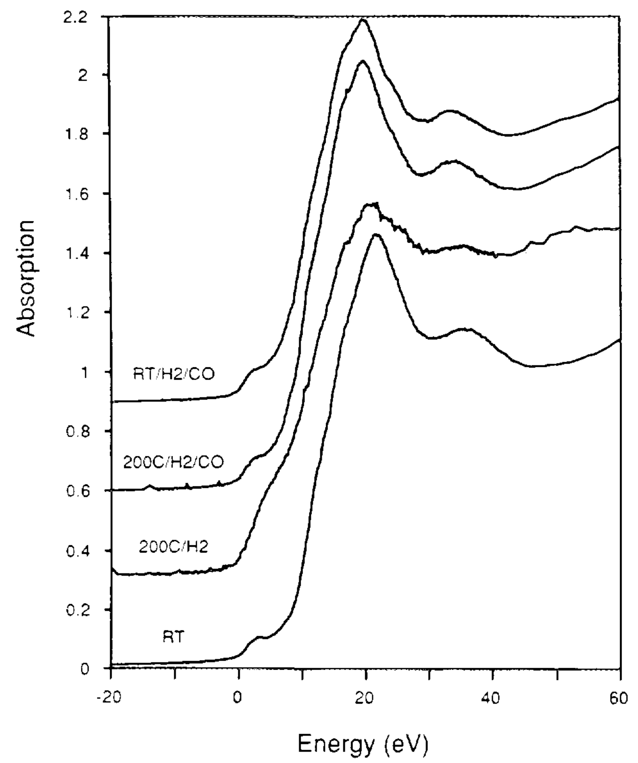

FIG. 7. *In situ* Co K-edge XANES spectra of the K–Co/Al_2O_3 catalyst (4.4 wt% Co, with K/Co ~1).

Cobalt K-Edge EXAFS

The extended X-ray absorption fine structure (EXAFS) region of the spectra were analyzed using standard data analysis procedure (14). The EXAFS χ spectrum was first Fourier transformed from k space to r space to obtain the radial structure function (RSF). The χ spectrum for one or several coordination shells was then isolated by inverse transform of the RSF at the appropriate region and subsequently fitted using the single scattering EXAFS equation (14). The RSFs for Co metal and Co_3O_4 are shown in Fig. 9. The coordination numbers (N) and interatomic distances (R) for the coordination shells of Co in the model compounds are listed in Table 1, together with those for CoO, which has the NaCl structure. The *in situ* EXAFS RSFs for the K–Co/Al_2O_3 and Co/Al_2O_3 catalysts are shown in Figs. 10 and 11, respectively. To obtain the structural parameters for the samples, inverse transforms for the Co shell from Co metal

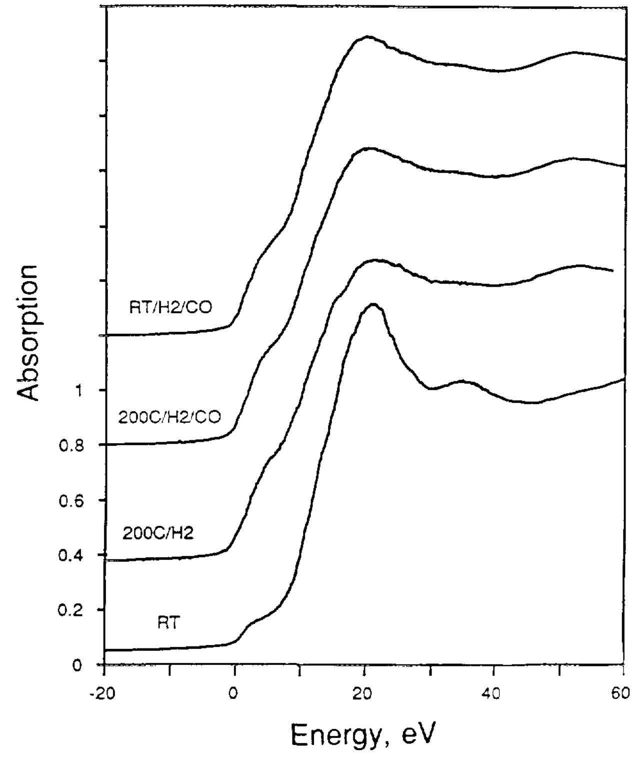

FIG. 8. *In situ* Co K-edge XANES spectra of the Co(9 wt%)/Al_2O_3 without K.

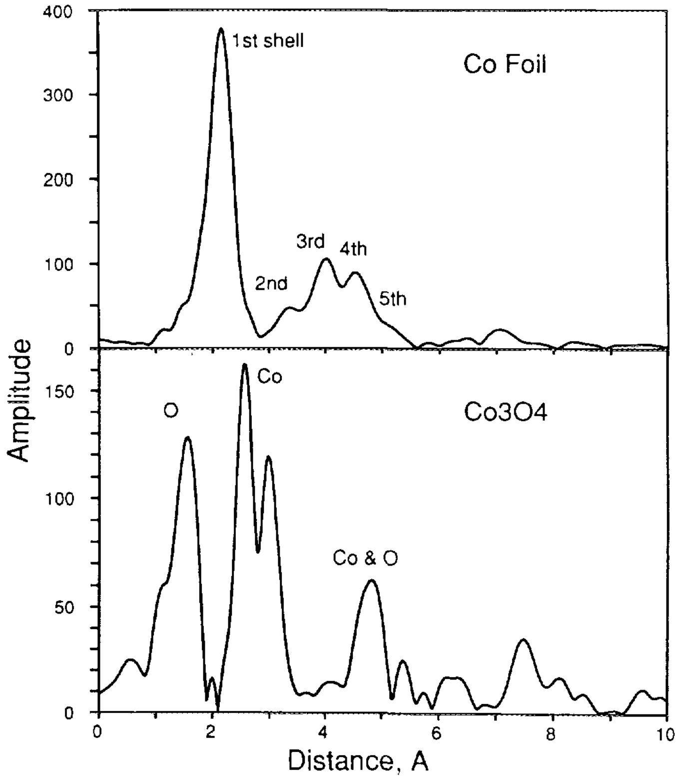

FIG. 9. EXAFS RSF of the Co K-edge for Co metal and Co_3O_4.

TABLE 1

Interatomic Distances (*R*) and Coordination Numbers (*N*) for the Co Model Compounds

Sample	*R*(Å)	*N*
Co metal		
Co–Co	2.51	12
Co–Co	3.57	6
Co–Co	4.36	24
Co–Co	5.02	12
Co–Co	5.62	24
Co_3O_4		
Co–O	1.81	1.33
Co–O	1.99	4
Co–Co	2.87	4
Co–Co	3.35	8
CoO		
Co–O	2.13	6
Co–Co	3.02	12
Co–O	3.69	8
Co–Co	4.27	6

and the oxygen shell from Co_3O_4 were first least-square fitted to extract the scattering amplitude and phase shift functions. These functions were then transferred as constants for fitting the inverse transforms for the catalysts (14). The catalysts usually contain more than one phase which are not well resolved in their RSFs. Therefore, the inverse transforms usually consist of two coordination shells and the fittings involve parameters for both shells. The structural parameters obtained from the least-squares fittings are summarized in Table 2. The EXAFS χ spectrum and the least-square fitting of the inverse transform for the two nearest oxygen shells of the K–Co/Al_2O_3 catalyst are shown in Figs. 12 and 13, respectively.

It is noted that the Co in Co_3O_4 is coordinated on average by 1.33 oxygens at 1.81 Å and 4 oxygens at 1.99 Å (Table 1). Since these two shells are not well separated in RSF (Fig. 9), we fitted them with one-shell parameters, assuming that the shell contains disorder, i.e., a larger value of Debye–Waller (D–W) coefficient compared with that for a single shell. For this reason, negative $\Delta\sigma^2$ values were obtained for the samples fitted with two-shell parameters (Table 2). The uncertainty in the coordination numbers (ΔN) has not been indicated in Table 2. In the most desirable case, for which the least-squares fitting involves only a single coordination shell which is well separated from its neighboring shells, ΔN is usually less than 20% (15). ΔN increases as the calculation involves more than one shell and is extended to the coordination shells beyond the nearest shells. Therefore, in our case, ΔN must be significantly larger than 20%. However, no attempt was made to quantitatively determine the distribution of the phases, which requires accurate N values.

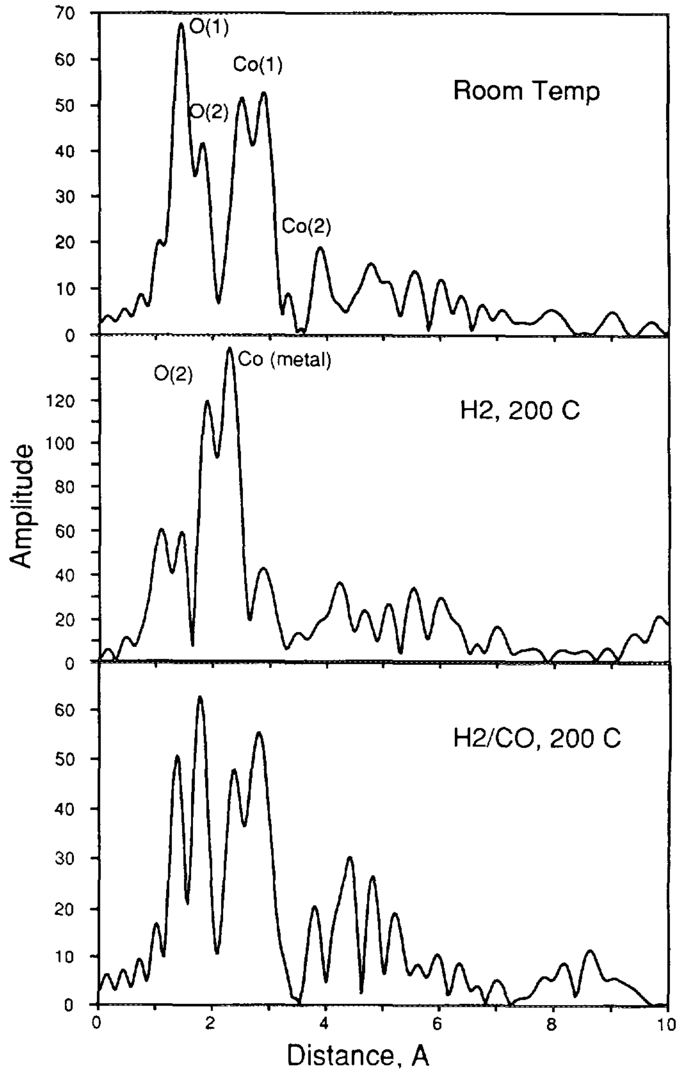

FIG. 10. *In situ* EXAFS RSFs for the K–Co/Al_2O_3 catalyst (9 wt% Co, with K/Co ~1), where O(1) is for Co_3O_4 and O(2) for CoO.

The RSF of the K-promoted Co/Al_2O_3 catalyst at room temperature shows two peaks at $R < 2$ Å (Fig. 10). Due to the scattering phase shift, these two peaks actually represent two oxygen shells at 1.96 and 2.12 Å, corresponding to the nearest O shells for Co_3O_4 and CoO, respectively (Table 2). The oxygen shell at 1.81 Å for Co_3O_4 is ignored in the calculation (Table 1) because the coordination number for the shell is expected to be < 1 (Co is present in two phases), which is within the uncertainty of the calculation. The RSF for the same sample shows two peaks at 2.1–3.2 Å, which are mainly contributed by the Co shells (Fig. 10). As compared with the RSF for Co_3O_4 (Fig. 9), the second peak is enhanced because of the Co shell at 3.02 Å from CoO (Table 1). To

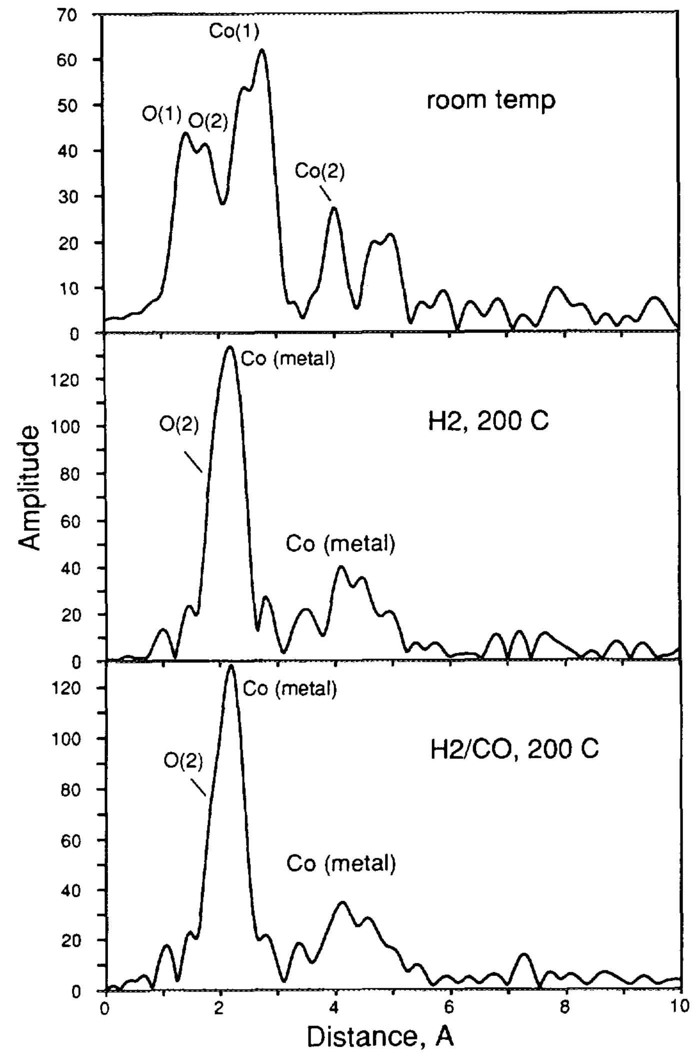

FIG. 11. *In situ* EXAFS RSFs for the Co/Al_2O_3 catalyst (9 wt% Co), where O(1) is for Co_3O_4 and O(2) for CoO.

avoid the complication of three-shell fitting, the inverse transform is fitted with a two-shell model and the second shell at 3.30 Å is attributed to a Co shell at 3.02 Å for CoO and a Co shell at 3.35 Å for Co_3O_4. At 200°C in H_2, the RSF shows a peak at ~2.3 Å representing a Co shell at 2.57 Å, which is within the experimental error of the nearest Co shell at 2.51 Å for Co metal (Fig. 9 and Table 1). The peak at ~1.9 Å in the RSF is attributed to an oxygen shell at 2.16 Å which is close to 2.13 Å for the nearest O shell for CoO. The weak peak at 1.4 Å indicates a small amount of Co_3O_4 (Fig. 10). The peak at 1.1 Å arises from the noise and does not represent a coordination shell. The result indicates that Co_3O_4 in the sample has been reduced largely to a mixture of Co metal and CoO. This finding is consistent with the results obtained from the corresponding XANES spectra (Fig. 7). At 200°C in H_2/CO, oxidation of Co occurs. EXAFS analysis indicates that the Co is present as Co_3O_4 and CoO (Fig. 10, Table 2).

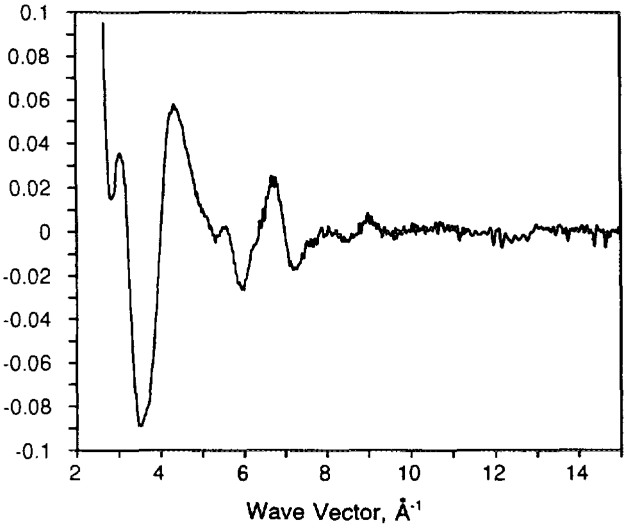

FIG. 12. EXAFS χ spectrum of the K–Co/Al_2O_3 catalyst (9 wt% Co, K/Co ~1) at room temperature.

The RSF for the Co/Al_2O_3 catalyst without K indicates that the catalyst is initially a mixture of CoO and Co_3O_4 (Fig. 11, Table 2) and is reduced to Co metal under H_2. The RSF shows no significant structural change in H_2/CO at 200°C. A small shoulder at < 2 Å in the RSF may indicate trace of an oxide phase. These results are also consistent with those obtained from the XANES spectra (Fig. 8). Because the EXAFS signal for the oxygen shell

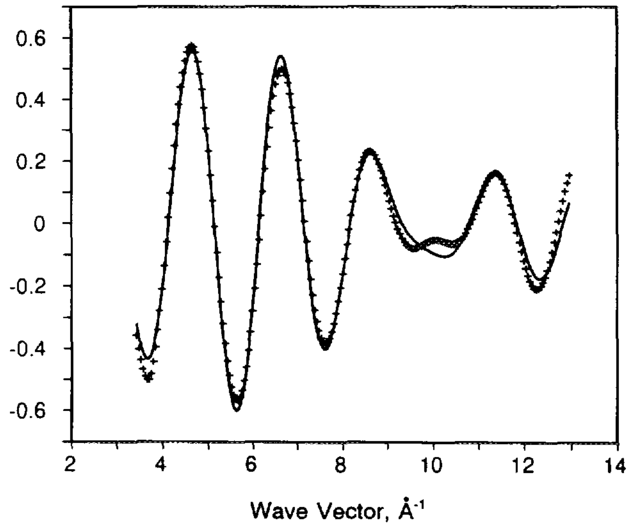

FIG. 13. Least-square fitting of the inverse-transform of the nearest two oxygen shells for the K–Co/Al_2O_3 catalyst (9 wt% Co, K/Co ~1) at room temperature. The solid line represents the experimental data.

TABLE 2

Interatomic Distances (R), Coordination Numbers (N), $\Delta\sigma^2$ (the Difference of the Debye–Waller (D–W) Coefficients between the Sample and the Standard), Regions for Inverse Fourier Transform, and Phases for the 9 wt% Co/Al_2O_3 Catalysts Promoted with K or without K

	R(Å) (± 2%)	N	$\Delta\sigma^{2a}$	Region for inv. trans (Å)	Phase
K–Co/Al_2O_3, R.T					
Co–O	1.96	2.6	−0.004	1.2–2.1	Co_3O_4
Co–O	2.12	2.8	−0.003	1.2–2.1	CoO
Co–Co	2.82	1.1	0.00	2.1–3.2	Co_3O_4
Co–Co	3.30	4.2	0.00	2.1–3.2	Co_3O_4, CoO
Co–Co	4.17	—	—	3.6–4.1	CoO
K–Co/Al_2O_3, H_2, 200°C					
Co–O	2.16	2.0	−0.003	1.6–2.6	CoO
Co–Co	2.53	4.5	−0.0002	1.6–2.6	Co metal
K–Co/Al_2O_3, H_2/CO, 200°C					
Co–O	1.96	1.7	−0.002	1.6–2.7	Co_3O_4
Co–O	2.12	2.5	−0.003	1.6–2.7	CoO
Co/Al_2O_3, R.T					
Co–O	1.94	2.1	−0.001	1.2–2.1	Co_3O_4
Co–O	2.11	3.3	0.0002	1.2–2.1	CoO
Co–Co	2.78	1.5	0.0	2.1–3.2	Co_3O_4
Co–Co	3.24	4.2	0.0	2.1–3.2	Co_3O_4, CoO
Co–Co	4.32	—	—	2.8–3.4	CoO
Co/Al_2O_3, H_2, 200°C					
Co–Co	2.50	6.3	0.0005	1.6–3.0	Co metal
Co–Co	4.35	6.1	0.0	3.8–4.4	Co metal
Co/Al_2O_3, H_2/CO, 200°C					
Co–Co	2.49	5.4	0.0005	1.7–3.0	Co metal
Co–Co	4.37	5.5	0.0	3.6–4.4	Co metal

[a] To simplify the calculation, for fitting the coordination shells beyond the nearest oxygen shell(s), the D–W coefficient is fixed at the values for the standard ($\Delta\sigma^2 = 0$).

is quite weak, it is not included in the least-squares fitting.

It is noted that the coordination numbers of the reduced Co catalysts are less than those for bulk Co metal (Table 2), suggesting the formation of small Co particles. For a sufficiently small particle, a large fraction of the atoms resides at the particle surface. These surface atoms have fewer nearest neighboring atoms. Thus, the average coordination number for a small particle is expected to be less than that for a bulk material. By assuming spherical particles and using the geometrical shape model by Greegor and Lytle (16), we estimate the average Co particle size of the reduced samples could be as small as 10–20 Å. It is noted, however, that the particle size estimated from the average coordination number by EXAFS analysis tends to be smaller than the actual size (17, 18). Furthermore, the EXAFS spectra for the model compounds, Co metal and Co_3O_4, were collected using transmission mode whereas the *in situ* measurements were made using fluorescence mode. The fluorescence mode often causes a reduction of the scattering amplitude due to self-absorption. For all of these reasons, the actual particle size is likely to be larger than 20 Å.

IV. SUMMARY AND CONCLUSIONS

In situ XAFS spectroscopy studies have been conducted at reaction conditions on potassium-promoted cobalt catalysts supported on SiO_2 and Al_2O_3 and on similar samples without potassium. Measurements were performed at temperature up to 200°C under both reducing (flowing H_2) and simulated F–T reaction (flowing CO/H_2) conditions. The results are summarized below.

1. Potassium K-edge and cobalt K-edge XANES spectra indicate that the K interacts with both the Co phase and SiO_2. The potassium promotion inhibits reduction of Co/SiO_2 in H_2 at 200°C. This has recently been found to be due to secondary aqueous impregnation and drying of

reduced and passivated Co/SiO_2 which leads to enhanced Co silicate formation (19). It is interesting to note that, in the presence of added water vapor during CO hydrogenation (equivalent to operating at high CO conversions), there is little difference between the states of the cobalt in the unpromoted and in the K-promoted catalysts since the unpromoted catalyst becomes more oxidized while the K-promoted catalyst does not apparently change significantly.

2. The Co in the K-promoted Co/Al_2O_3 catalyst is initially present as a mixture of Co_3O_4 and CoO. Under H_2 at 200°C, it is reduced to a mixture of CoO and Co metal. During reaction at 200°C in H_2/CO, it is converted to a mixture of Co_3O_4 and CoO. The results indicate that the K-promoted Co/Al_2O_3 catalyst is less able to be reduced than the unpromoted catalyst, perhaps for a reason similar to that cited above.

3. Without potassium, both the Co K-edge XANES and EXAFS RSFs for the Co/Al_2O_3 catalyst show that the Co is reduced almost completely to Co metal under H_2 at 200°C, and remains in that form during reaction at 200°C in H_2/CO. Only a minor trace of Co oxide is observed.

4. The presence of K in the Co/Al_2O_3 catalysts leads to more oxidation of the catalyst during CO hydrogenation.

ACKNOWLEDGMENT

The work presented here was financially supported by the National Science Foundation (Grant CBT-8715541).

REFERENCES

1. Guszi, L., and Làzàr, K., *Catal. Lett.* **7,** 53 (1990).
2. Butt, J., *Catal. Lett.* **7,** 61 (1990).
3. Chuang, S. S. C., and Pien, S. I., *J. Catal.* **135,** 618 (1992).
4. Gupta, N. M., Kamble, V. S., Iyer, R. M., Thampi, K. R., and Grätzel, M., *J. Catal.* **137,** 473 (1992).
5. McQuire, M. W., and Rochester, C. H., *J. Catal.* **141,** 355 (1993).
6. Sinfelt, J. H., *in* "Bimetallic Catalysts." Wiley, New York, (1983).
7. Lytle, F. W., Via, G. H., and Sinfelt, J. H., *in* "Synchrotron Radiation Research" (H. Winick and S. Doniach, Eds.), p. 401. Plenum, New York, 1980.
8. Clausen, B. S., Topsøe, H., and Candia, R., *J. Phys. Chem.* **85,** 3868 (1981).
9. Huffman, G. P., Huggins, F. E., Jenkins, R. G., Lytle, F. W., and Greegor, R. B., *Fuel* **65,** 1339 (1986).
10. Huggins, F. E., Shah, N., Huffman, G. P., Jenkins, R. G., Lytle, F. W., and Greegor, R. B., *Fuel* **67,** 938 (1988).
11. Huffman, G. P., Ganguly, B., Zhao, J., Rao, K. R. P. M., Shah, N., Feng, Z., Huggins, F. E., Taghiei, M. M., Lu, F., Wender, I., Pradhan, V. R., Tierney, J. W., Seehra, M. S., Ibrahim, M. M., Shabtai, J., and Eyring, E. M., *Energy Fuels* **7,** 285 (1993).
12. Lytle, F. W., Wei, P. S. P., Greegor, R. B., Via, G. H., and Sinfelt, J. H., *J. Chem. Phys.* **70,** 4849 (1979).
13. Lytle, F. W., Greegor, R. B., Marques, E. C., Sandstrom, D. R., Via, G. H., and Sinfelt, J. H., *J. Catal.* **95,** 546 (1985).
14. Sayers, D. E., and Bunker, B. A., *in* "X-Ray Absorption: Principles, Applications, Techniques of EXAFS, SEXAFS and XANES" (D. C. Koningsberger and R. Prins, Eds.), Wiley, New York (1988).
15. Eisenberger, P., and Lengeler, B., *Phys. Rev. B* **22,** 3351 (1980).
16. Greegor, R. B., and Lytle, F. W., *J. Catal.* **63,** 476 (1980).
17. Zhao, J., and Montano, P. A., *Phys. Rev. B* **40,** 3401 (1989).
18. Ashcroft, A. T., Cheetham, A. K., Harris., P. J. F., Jones, R. H., Natarajan, S., Sankar, G., Stedman, N. J., and Thomas, J. M., *Catal. Lett.* **24,** 47 (1994).
19. Haddas, G., and Goodwin, J. G., Jr., to be submitted.